Supplementary Information (SI) for Physical Chemistry Chemical Physics.
This journal is © the Owner Societies 2025

Fig. S1 illustrates the experimental and calculated Raman spectra of $Zn_2Mo_3O_8$ and the schematic representation of the stretching vibration of the Mo cluster corresponding to the A_1 vibrational mode around 439 cm^{-1}.

Fig. S2 and Fig. S3 respectively present the thermal activation model fitting results for $Zn_2Mo_3O_8$ and $Fe_2Mo_3O_8$, utilizing electrical transport data ranging from 250 K to 300 K.

Fig. S4 illustrates the pressure-dependent resistivity of $Fe_2Mo_3O_8$ and $Zn_2Mo_3O_8$, with solid circles representing compression and hollow circles representing decompression. The resistivity of both compounds decreases gradually with increasing pressure, and the trend slows down over time. Additionally, during the decompression process, the resistivity is consistently lower compared to the resistivity at the same pressure during the compression process.

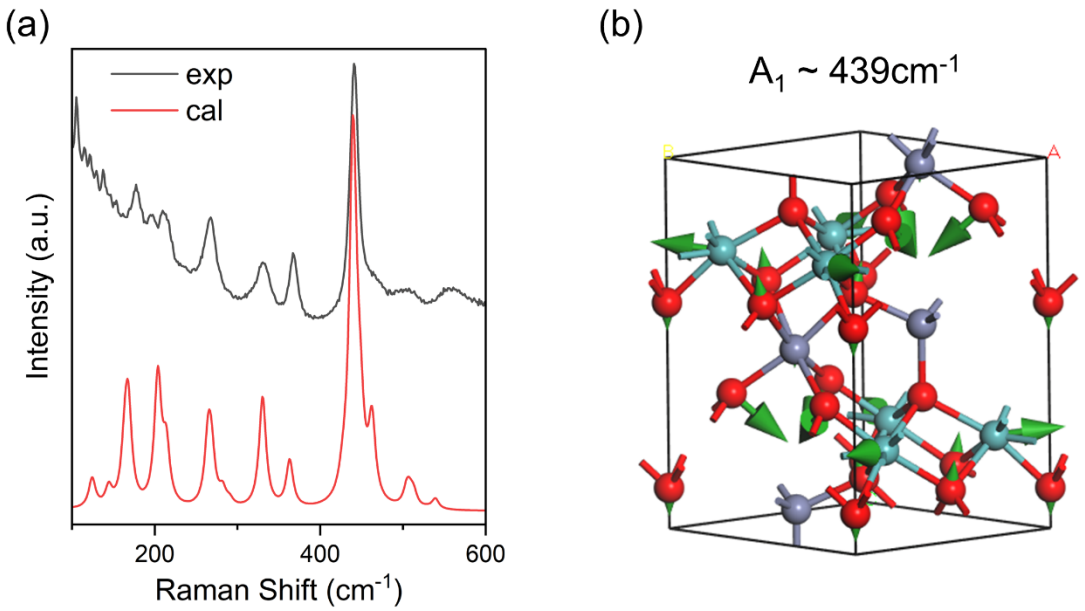

Figure S1. (a) The experimental and calculated Raman Spectra of Zn2Mo3O8. (b) The schematic representation of the stretching vibration of the Mo_3 cluster corresponding to the A_1 vibrational mode around 439 cm^{-1} based on the computational results.

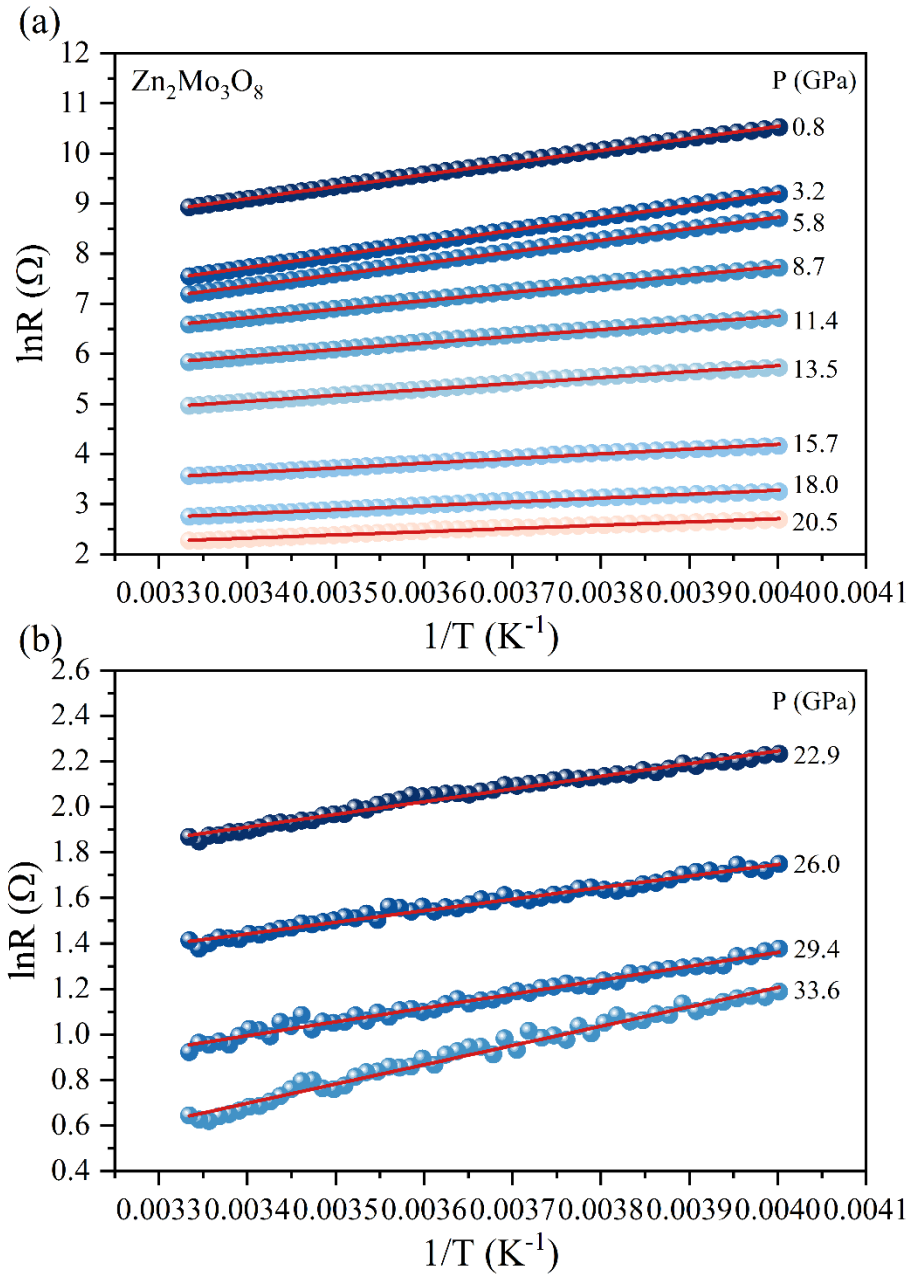

Figure S2. The result of thermal activation model fitting of $Zn_2Mo_3O_8$.

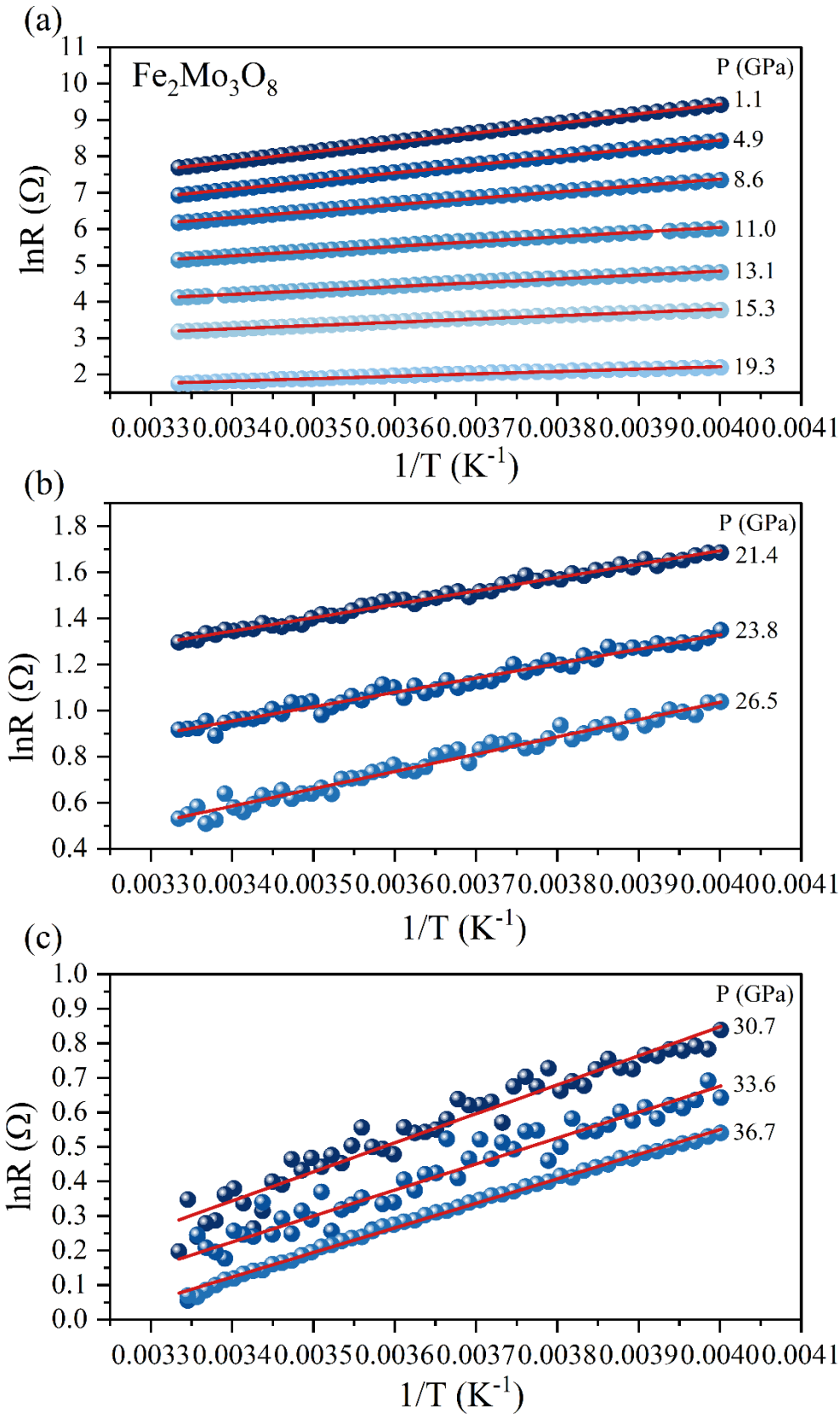

Figure S3. The result of thermal activation model fitting of $Fe_2Mo_3O_8$.

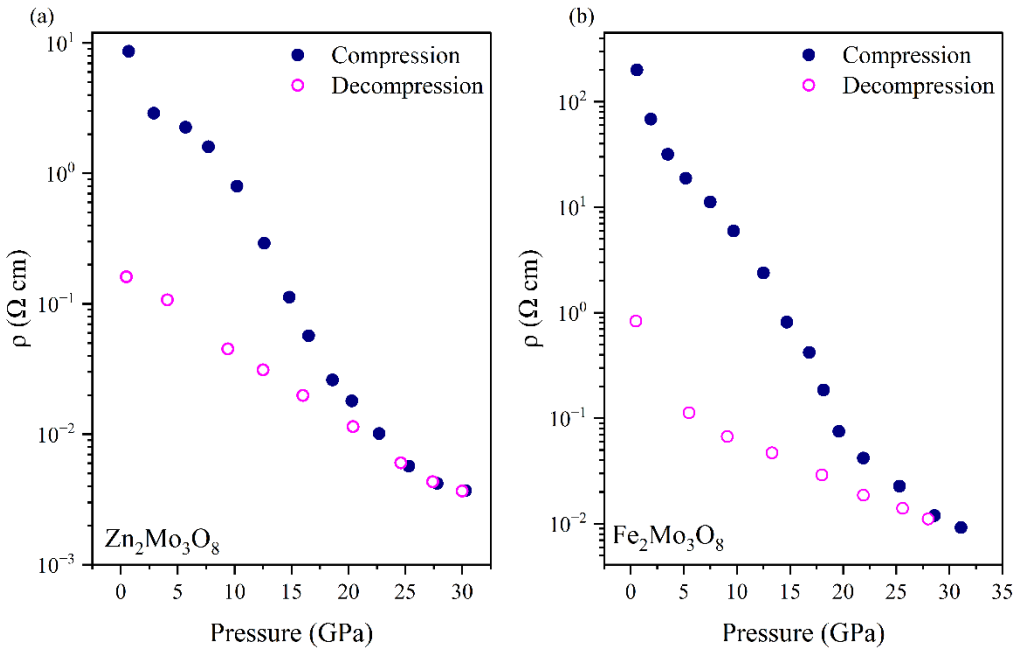

Figure S4. Pressure-dependent resistivity of (a) $Zn_2Mo_3O_8$ and (b) $Fe_2Mo_3O_8$.